A sigma-delta interface built-in self-test and calibration for microelectromechanical system accelerometer's utilizing interpolation method

Anwer Sabah Ahmed[1,2], Qais Al-Gayem[2]
[1]Technical Institute of Al-Najaf, Al-Furat Al-Awsat Technical University, Najaf, Iraq
[2]Electrical Engineering Department, College of Engineering University of Babylon, Babil, Iraq

Article Info	**ABSTRACT**

This work presents the capacitive micromechanical accelerometer with a completely differential high-order switched capacitor sigma-delta modulator interface. Such modulation interface circuit generates one-bit output data using a third sigma-delta modulator low-noise front-end, doing away with the requirement for a second enhanced converter of resolution to encode the feedback route analog signal. A capacitive micromechanical sensor unit with just a greater quality factor has been specifically employed to give greater resolution. The closed-loop and electrical correction control are used to dampen the high-Q values to get the system's stability with high-order. This microelectromechanical system (MEMS) capacitive accelerometer was calibrated using a lookup table and Akima interpolation to find manufacturing flaws by recalculating voltage levels for the test electrodes. To determine the proper electrode voltages for fault compensation, COMSOL software simulates a number of defects upon that spring as well as the fingers of the sensor system. When it comes time for the feedback phase of a proof mass displacement correction, these values are subsequently placed in the lookup table.

Corresponding Author:

Anwer Sabah Ahmed
Najaf technical Institute, Al-Furat Al-Awsat Technical University
Al-Najaf 31001, Iraq
Email: anwar.altamimi@student.uobabylon.edu.iq

1. INTRODUCTION

Inertial navigation and guiding, navigation for such consumer markets, weightless studies in spacecraft, inclination adjustment, or platform stability are all using high-precision capacitive accelerometer sensors of µg resolution [1]. A reduced noise sensor element and the interface are essential components of such an increased resolution sensor system. The interface typically sets a limit on the overall system resolution, especially for high-Q sensing elements with low Brownian noise floors. On the other hand, in order for high-quality transducers with vacuum packaging to be useful as sensors, they must first be electronically damped. The sensing element is constrained in the sense the frequency band, input range, and damping because there is not a force in the feedback to modify the displacement related to acceleration of the transfer function [2]. It has been established that closed-loop operation increases the linearity, dynamic range, as well as frequency range of capacitive accelerometers. A high-Q sensor unit can be electrically made under-damped using a closed-loop architecture without unnecessary complexity, which is not achievable with an open-loop system [3]–[5]. Gyroscope and accelerometer applications, among others, have benefited from the sigma-delta modulation technique used in analog-to-digital converters [6]–[9]. Closed-loop sigma-delta capacitive accelerometers may create high output data, and electrostatics feedback insulates the sensor from the effects of process fluctuations, resulting in a more

stable and precise system [10]. An electromechanical closed-loop system's noise-shaping ability can be improved by using interpolation for the fault diagnostic and compensation.

In this method, we can manipulate a wide range of fingers and the spring fault resulted because of aging or manufacturing. Lajevardi *et al*. [9] did not, however, give a thorough circuit design. In [11], the increased order of the closed-loop microelectromechanical sigma-delta modulator with both higher sensitivity and low-quality factor accelerometer was developed, resulting in an inherent system with a more stable state. Additionally, this system (closed loop) did not achieve sub-g equivalent resolution during testing. This continuous-time capacitive accelerometer interfacing using a high-Q mechanical element was disclosed in [4], [12] with sub-g comparable resolutions. An incredibly low-noise accelerometer, but still no thorough circuit design method, is presented in [13], [14] proposes a low-frequency impedance-based approach for identifying damaged array components, which is supported by actual electrode array readings for drug testing on cardiac and neuronal tissue. The array comprising nanoscale electromechanical switches is designed, put into practice, and tested in article 15 utilizing an online test that makes use of the superposition principle. Using MATLAB-Simulink as well as OrCAD PSpice programs were used to implement various simulations of these switches [15], [16] offers two methods for identifying electrode degradation at their interfaces with fluidic and biological systems. All these mentioned papers did not manipulate a wide variety of faults and damages as a result of aging or manufacturing. Therefore, our work is aimed at this purpose.

2.   COMB DRIVE AND BROWNIAN NOISE

Because of the greater power signal, low-temperature sensitivity, with simplicity in providing electrostatic force to enable closed-loop control, a capacitive microelectromechanical systems (MEMS) accelerometer is selected as the front-end sensor device [17], [18]. The mechanical transfer function can be calculated using Newton's Second Law (1).

$$H_{ms} = \frac{x}{a} = \frac{1}{S^2 + \frac{b}{m}S + \frac{k}{m}} = \frac{1}{mS^2 + \frac{m\omega_0}{Q}S + k} \tag{1}$$

where m is the proof mass, b is the damping factor, k is the spring constant, ω_0 represents the resonate frequency, and Q represents the quality factor. The system's response in a closed-loop topology is the result of adding all responses of the interface circuit and the sensing element. As a result, the system's bandwidth, sensitivity, and resonance characteristics are no longer dominated by the aforementioned parameters, increasing the freedom of mechanical parameter choices.

Brownian noise, which would be produced by the motion of the suspension beam and gas molecules, is the principal source of noise in the mechanical component. These steps are used to determine Brownian noise equivalent acceleration (BNEA).

$$BENA = \frac{\sqrt{4k_b T_b}}{9.8m} \quad \left[g \middle/ \sqrt{Hz} \right] \tag{2}$$

T_b is the temperature in Kelvin, and k_b is the Boltzmann constant. Two effective methods for producing a low BNEA include expanding the size of a proof mass and reducing air damping [17], [19], [20]. Brownian noise is reduced when this sensor is operated in a vacuum environment but at the expense of a lengthy settling period and poor antishock capabilities [21]–[25]. The vacuum-packaged sensor element used in this study in modeling and measurement really does have an open-loop basic resonance of 1 kHz. The sensor quality factor is greater than 40, as well as the BNEA is less than 60 ng/√H. The sensor element's corresponding static capacitance and sensitivity are 180 pF and 10 pF, respectively.

3.   THE METHOD OF CALIBRATION

For the movement of the proof mass as though the applied acceleration (50 g), the estimates of left and right testing voltages (VL and VR, respectively) in COMSOL software can be utilized to determine the necessary amount of the built-in self-test (BIST) (DC test voltage), namely VL and VR. The output is then compared to the intended outputs (Y1, Y2, Y3, ..., Yn) that were determined by COMSOL and saved in a lookup table as depicted in Figure 1 to use against the Akima interpolation. The output is then decided to apply to such a corrected test electrode to even get displacement for the proof mass to really get output equivalent when acceleration is +50 g. The computed VR is delivered to a fixed test electrode in a similar manner to provide an output that is equivalent to that when the acceleration is (-50 g). Nothing will be made unless the 's results are satisfactory. If not, a lookup table will determine the voltage that will serve as feedback in order to compensate (calibrate) for the error that occurred.
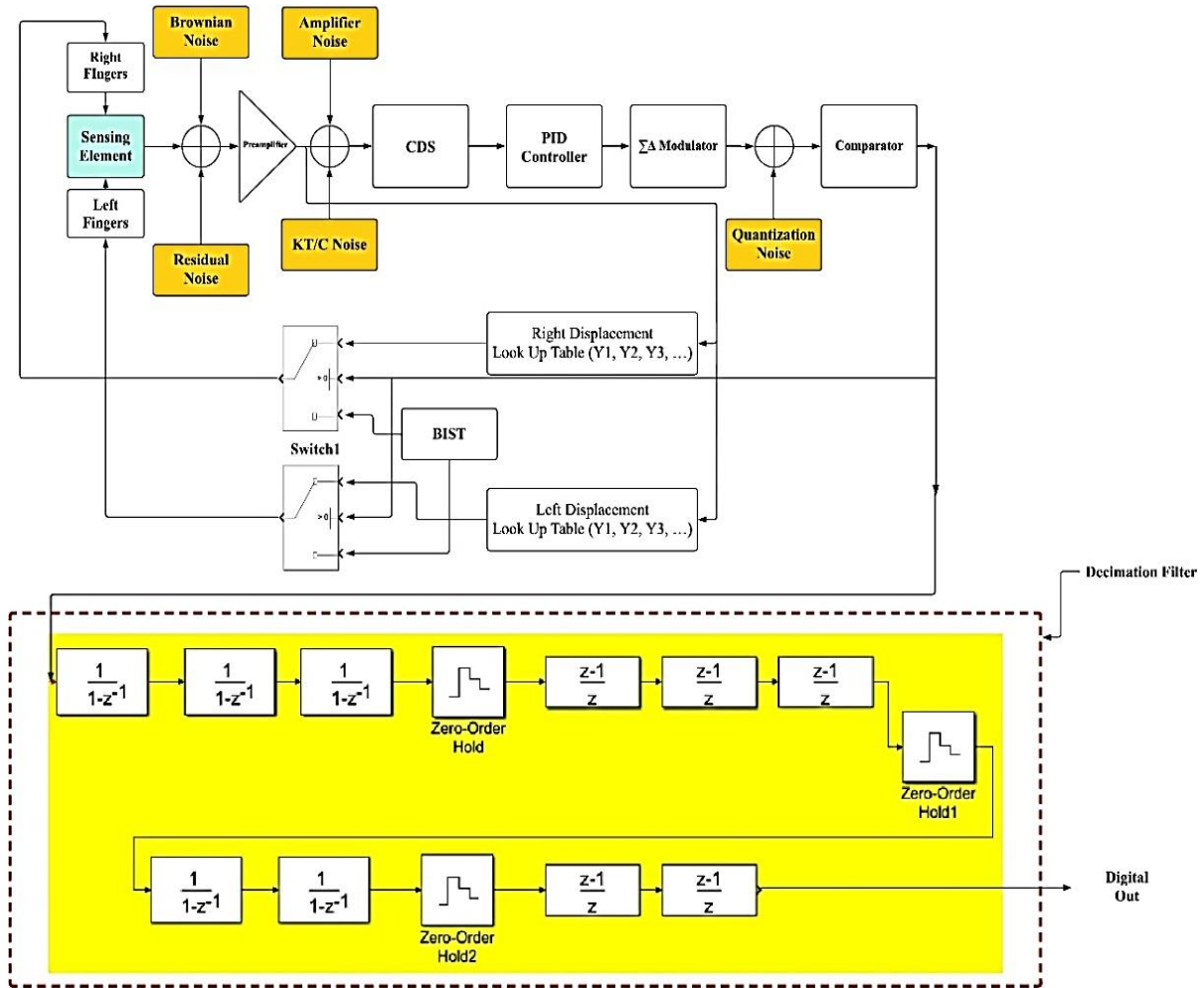
Figure 1. The proposed self-test and calibration system

In applied mathematics, the Akima spline is just a non-smoothing spline that provides strong fits for curves having rapidly fluctuating second derivatives. When given a certain set of "knot" endpoints, an Akima spline will traverse all of the points (x_i, y_i) where the (x_i) strictly are growing. Its slope, s_i, depends on the locations of its endpoints (x_{i-2}, y_{i-2}) at those points through (x_{i+2}, y_{i+2}). A reference line's slopes over (x_i, y_i) until (x_{i+1}, y_{i+1}) are specified as mi. Then, similar to (3), the weighted mean for m_{i-1} and m_i is used to determine s_i.

$$s_i = \frac{|m_{i-1}-m_i|m_{i-1}+|m_{i-1}-m_{i-2}|m_i}{|m_{i-1}-m_i|+|m_{i-1}-m_{i-2}|} \tag{3}$$

The spline is thus defined as a piece-wise cubic function whose value between xi and xi-1 is the single cubic polynomial $PL(x_i)$ which meets all four restrictions: $PL(x_i) = y_i$, $L(x_{i+1})=y_{i+1}$, $PL'(x_i)=s_{i+1}$. The Akima spline has the advantage of only using data from adjacent knot points when constructing overall parameters of interpolated polynomials at between the two-knot points. This eliminates the need to solve a complex system of equations, and the Akima spline prevents unphysical wiggles in locations where the underlying curve's second derivative is quickly changing. The Akima spline has the advantage of only using data from adjacent knot points when constructing the overall parameters of interpolated polynomials in between two-knot points.

4. DECIMATION FILTER MODEL

To eliminate the unwanted data and for filtering out the noise of the high frequency at the output, sinc filters are utilized as decimation filters. A two-stage cascaded decimation filter was used to create this decimation filter. The electromechanical sigma-delta system employed in this work has an order of 2, hence the sinc filter must have an order of at least 3. As a result, in the first stage of the filter, a 3rd order sinc filter is

employed, and a 2nd order sinc filter is used to filter the noise even further in the second stage, as illustrated in Figure 1. Sinc filters are constructed of blocks used for both addition and subtraction operations with (4) and (5) transfer functions which is a low pass filter, respectively.

$$\frac{Y(Z)}{X(Z)} = \frac{1}{1-Z^{-1}} \tag{4}$$

$$\frac{Y(Z)}{X(Z)} = 1 - Z^{-1} \tag{5}$$

The readout circuit's comparator output provides the input bitstream, which is a 1-bit digital data stream. Because N_d is set to 40, the 3rd order decimation filter's output is a number that may be written as a 16-bit digital value, as determined by (6).

$$p = M_d \log_2 N_d + B \tag{6}$$

M_d represents the decimation filter degree, Nd represents the decimation order, B is the bits number of the word at the input, and p is the number of bits of the word in the output.

Both M_d (degree of decimated filter) and N_d (decimation order) parameters are crucial in sinc filter design. The degrees of the closed-loop electromechanical sigma-delta system determine M_d, while the required bandwidth of the system specifies N_d. The degree of the sinc filter should be at least just a little more than the degree of the closed loop electromechanical sigma-delta system [24], [25] to produce a low noise output. The noise at higher frequencies is filtered again as the degrees of the sinc filter grow because the size of the filter's ripple at high frequencies reduces.

5.   FEEDBACK FORCE

In closed-loop activities, the feedback path affects system performance as long as the loop gain is large enough. The only component of the feedback loop in our system is the electrostatic feedback force, and the electrical BIST stimulus is turned into a physical actuation force. As a result, important system attributes such as sensitivity, linearity, and dynamic range are significantly affected. When a voltage drop (V) is applied to both sensor plates, an electrostatic force of attraction is formed between them, which is given by (7) [4],

$$F_{electrostatic} = \frac{C_o d_o V^2}{2(do+x)^2} \tag{7}$$

where (d_0) is the initial distance between the plates, (C_0) is the static capacitance, and (x) is the displacement of the proof mass at that moment. This collocated sensing technology will reduce higher-order resonance phenomena while simplifying sensing element design [16], [24], [25].

6.   CIRCUIT NOISE SOURCES

The amplification noise, switching noise, referencing voltage noise, wire resistance noise, clocking fluctuation noise, and the noise of the mass residual motion are the principal sources of noise in the readout circuit [1]. The noise that belongs to the front amplifier, switching noise, the noise of reference voltage, plus noise of wiring resistance is the most significant noise sources in the proposed closed-loop interface. A single-ended simplified schematic for calculating overall circuitry noise equivalent acceleration (CNEA) is shown in Figure 2. Individually, these major noise sources are examined.
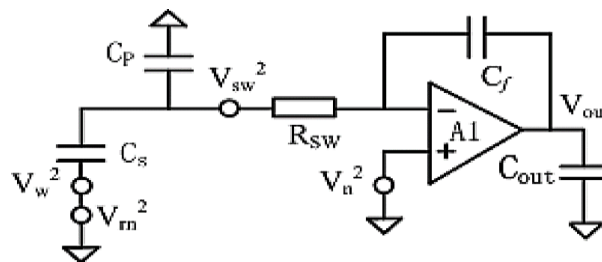

Figure 2. The overall circuitry of the noise equivalent acceleration

In Figure 2, C_s is the sensing capacitance, C_p is the capacitance because of the parasitism and C_f is the integrator feedback capacitance. The major sources of noise of the front-end amplifier are thermal noise and flicker noise, with flicker noise being minimized thanks to the use of the correlated double sampling (CDS) approach. The capacitive accelerometer's front-end gain in frequencies just below mechanical resonant frequency is given as (8).

$$V_{out} = \frac{4C_oV_S}{C_f d_o w_o^2} a(f)$$
(8)

The study demonstrates that its input referred noise induced by amplifier noise is bandwidth independent. This integrating capacitance should be reduced to reduce noise. By raising the sampling frequency and CDS capacitance, it is possible to reduce input referred noise. Raising both sensor capacitance and also reference voltage also is beneficial for making a high front-end circuit.

The reference voltages charge every sensor capacitor of both the low-noise front-end circuits in each cycle, and the reference voltage noise directly impacts the sensor readout output noise. Due to the sampling on the sensing capacitor, the wideband noise also was folded into the low-frequency region. The sensor interconnects series resistances contribute to the overall noises, and the wire resistance noise depicted in Figure 2 is combined into one equivalent resistance. This closed-loop operation amplifier bandwidth is limited, and the noise owing to wiring resistance is shown in [23].

7. CIRCUIT IMPLEMENTAION

The switched capacitor circuit is used to build the amplifier as presented in Figure 3. A charge amplifier converts the capacitance shift to voltages in the first stage. It has been successful. Lower frequencies of in-band noise and jitter were reduced using a CDS approach. The front-end amplifier's DC offset is considerably decreased. The phase lead compensation is put into action. with the help of a summing amplifier.

The CDS approach is used to reduce low-frequency signals with offsets in the front-end amplifier. Figures 4 and 5 depict the hold circuit and CDS implementation, respectively. To reduce the residue effect of prior feedback force, every electrode of the sensing device is linked to the ground during the reset phase. The feedback capacitor Cf is also depleted of its charge. The sensing element is then filled by a pair of supply voltages in phase A, and the switched capacitor circuit calculates and stores the differential capacitance changes on the capacitor CCDS. The polarity of the charging voltage of the sensing device is then inverted in phase B, resulting in a low voltage change (negative) just at the charge amplifier's output.
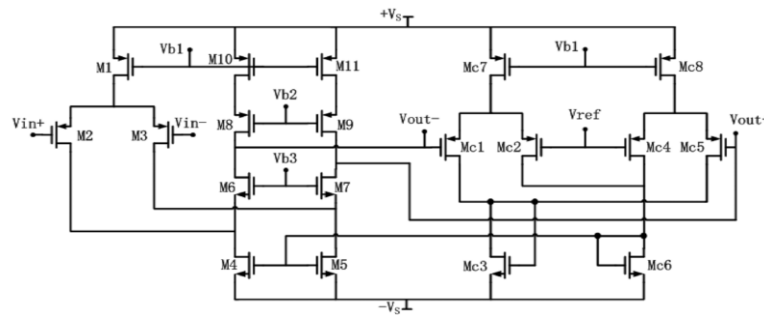

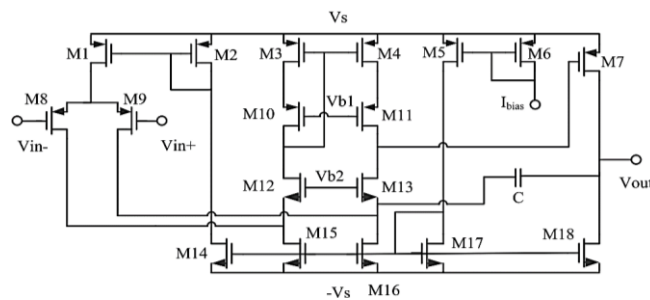Figure 3. The operation amplifier circuit using the switched capacitor

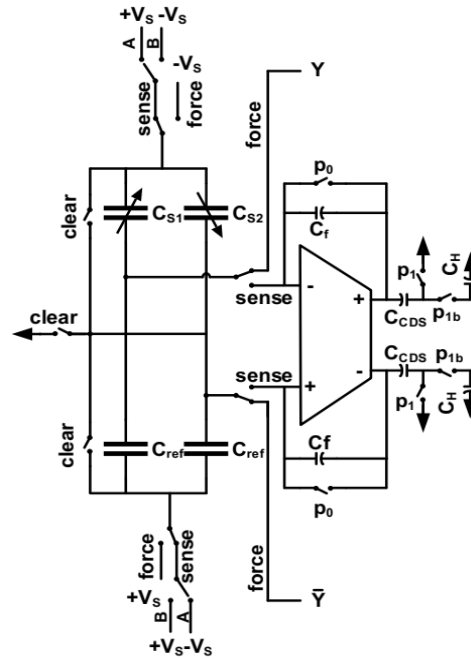Figure 4. The hold circuit using the switched capacitor

Figure 5. The CDS circuit with the switched capacitor

8. RESULTS AND DISCUSSION

In order to calculate the appropriate self-test electrode voltage to get the sensing element back to its pre-fault position, the lookup table was first provided with said intended referenced responses of the sensing device (spring and fingers fault-free case). Figure 6 displays the sigma-delta accelerometer's spectrum before and after it has been calibrated for a number of finger and spring defects, demonstrating effective correction. After each computation, Akima stores the computed voltage in the lookup table as one of the stored inputs for the upcoming self-test and calibration.
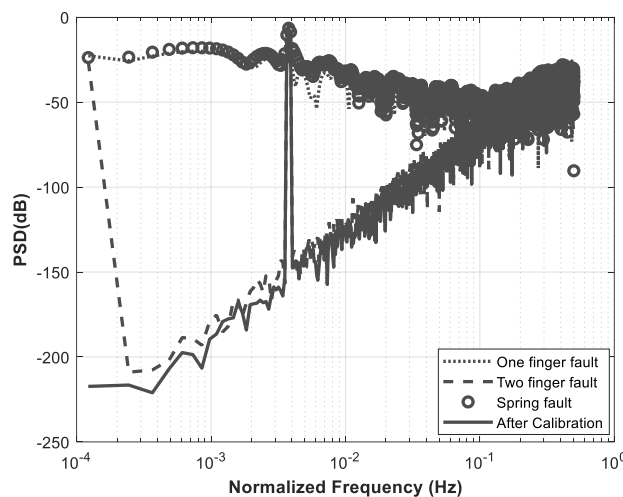

Figure 6. The spectrum output of the sigma-delta accelerometer for various finger and spring faults

9. CONCLUSION

The reduced noise (sigma-delta) accelerometer has been constructed and modeled in COMSOL and MATLAB for this paper. The comb drive was first flawlessly designed analytically. The design is then simulated, and COMSOL is used to generate the necessary BIST signal at (50 g) for something like the self-

test electrodes in order to identify the appropriate displacement for the test. To observe how the interpolation of Akima for the calibration was performed, several failure mechanisms for the fingers were tested in the comb drive. It was discovered that Akima interpolation was utilized to determine the required voltage in order to correct the sensor element's failure.

REFERENCES

[1] H. Kulah, J. Chae, N. Yazdi, and K. Najafi, "Noise analysis and characterization of a sigma-delta capacitive microaccelerometer," *IEEE Journal of Solid-State Circuits*, vol. 41, no. 2, pp. 352–361, Feb. 2006, doi: 10.1109/JSSC.2005.863148.

[2] A. S. Ahmed and Q. Al-Gayem, "Micro accelerometer built-in self-test and calibration using genetic algorithm and interpolation method," in *2022 IEEE International Conference on Semiconductor Electronics (ICSE)*, Aug. 2022, vol. 47, no. 7, pp. 49–52, doi: 10.1109/ICSE56004.2022.9863170.

[3] P. Kumari, K. Singh, and A. Singal, "Reducing the hygroscopic swelling in MEMS sensor using different mold materials," *International Journal of Electrical and Computer Engineering (IJECE)*, vol. 10, no. 1, pp. 494–499, Feb. 2020, doi: 10.11591/ijece.v10i1.pp494-499.

[4] A. S. Ahmed and Q. Al-Gayem, "Self-test and calibration methods for micro electro-mechanical systems," *TELKOMNIKA (Telecommunication Computing Electronics and Control)*, vol. 21, no. 1, p. 186, Feb. 2023, doi: 10.12928/telkomnika.v21i1.24251.

[5] L. Aaltonen and K. Halonen, "Continuous-time interface for a micromachined capacitive accelerometer with NEA of 4g and bandwidth of 300Hz," *Sensors and Actuators A: Physical*, vol. 154, no. 1, pp. 46–56, Aug. 2009, doi: 10.1016/j.sna.2009.07.011.

[6] N. Yazdi, F. Ayazi, and K. Najafi, "Micromachined inertial sensors," *Proceedings of the IEEE*, vol. 86, no. 8, pp. 1640–1659, 1998, doi: 10.1109/5.704269.

[7] E. Colinet, J. Juillard, S. Guessab, and R. Kielbasa, "Resolution enhancement of a sigma-delta micro-accelerometer using signal prediction," in *2004 International Conference on MEMS, NANO and Smart Systems (ICMENS'04)*, 2004, pp. 409–413, doi: 10.1109/ICMENS.2004.1508984.

[8] H. Zhang, X. Wei, Y. Ding, Z. Jiang, and J. Ren, "A low noise capacitive MEMS accelerometer with anti-spring structure," *Sensors and Actuators A: Physical*, vol. 296, pp. 79–86, Sep. 2019, doi: 10.1016/j.sna.2019.06.051.

[9] P. Lajevardi, V. P. Petkov, and B. Murmann, "A $\Sigma\Sigma\Delta$ interface for MEMS accelerometers using electrostatic spring constant modulation for cancellation of bondwire capacitance drift," *IEEE Journal of Solid-State Circuits*, vol. 48, no. 1, pp. 265–275, Jan. 2013, doi: 10.1109/JSSC.2012.2218721.

[10] J. Wu and L. R. Carley, "Electromechanical /spl delta//spl sigma/ modulation with high-Q micromechanical accelerometers and pulse density modulated force feedback," *IEEE Transactions on Circuits and Systems I: Regular Papers*, vol. 53, no. 2, pp. 274–287, Feb. 2006, doi: 10.1109/TCSI.2005.857084.

[11] I. Galton, R. Schreier, and G. C. Temes, "Book review: Delta-sigma data converters," *IEEE Solid-State Circuits Society Newsletter*, vol. 10, no. 3, pp. 5–6, Sep. 2005, doi: 10.1109/N-SSC.2005.6500102.

[12] B. Vakili Amini, R. Abdolvand, and F. Ayazi, "A 4.5-mW closed-loop ΔΣ micro-gravity CMOS SOI accelerometer," *IEEE Journal of Solid-State Circuits*, vol. 41, no. 12, pp. 2983–2991, Dec. 2006, doi: 10.1109/JSSC.2006.884864.

[13] L. Aaltonen, P. Rahikkala, M. Saukoski, and K. Halonen, "High-resolution continuous-time interface for micromachined capacitive accelerometer," *International Journal of Circuit Theory and Applications*, vol. 37, no. 2, pp. 333–349, Mar. 2009, doi: 10.1002/cta.547.

[14] H. Goldberg, J. Gannon, J. Marsh, B. Reichert, and M. Zavaleta, "An extremely low-noise MST accelerometer using custom ASIC circuitry," in *Proceedings Sensor Expo Fall*, 2000, pp. 479–482.

[15] Q. Al-Gayem, H. Liu, A. Richardson, and N. Burd, "Built-in test solutions for the electrode structures in bio-fluidic microsystems," in *2009 14th IEEE European Test Symposium*, May 2009, pp. 73–78, doi: 10.1109/ETS.2009.24.

[16] L. Mahdi and Q. Al-Gayem, "Design, simulation and testing of an array of nano electro mechanical switches (NEMS)," *Indonesian Journal of Electrical Engineering and Computer Science*, vol. 22, no. 1, pp. 113–120, Apr. 2021, doi: 10.11591/ijeecs.v22.i1.pp113-120.

[17] Q. Al-Gayem, H. Liu, A. Richardson, and N. Burd, "Test strategies for electrode degradation in bio-fluidic microsystems," *Journal of Electronic Testing*, vol. 27, no. 1, pp. 57–68, Feb. 2011, doi: 10.1007/s10836-010-5180-9.

[18] L. Aaltonen, P. Rahikkala, M. Saukoski, and K. Halonen, "Continuous time interface for ±1.5 g closed-loop accelerometer," in *2007 IEEE International Conference on Integrated Circuit Design and Technology*, May 2007, pp. 1–4, doi: 10.1109/ICICDT.2007.4299571.

[19] M. Pastre *et al.*, "A 300Hz 19b DR capacitive accelerometer based on a versatile front end in a 5th-order $\Delta\Sigma\Sigma$ loop," in *2009 Proceedings of ESSCIRC*, Sep. 2009, pp. 288–291, doi: 10.1109/ESSCIRC.2009.5326033.

[20] M. Yucetas, J. Salomaa, A. Kalanti, L. Aaltonen, and K. Halonen, "A closed-loop SC interface for a ±1.4g accelerometer with 0.33% nonlinearity and 2μg/vHz input noise density," in *2010 IEEE International Solid-State Circuits Conference - (ISSCC)*, Feb. 2010, pp. 320–321, doi: 10.1109/ISSCC.2010.5433899.

[21] S.-S. Tan, C.-Y. Liu, L.-K. Yeh, Y.-H. Chiu, M. S.-C. Lu, and K. Y. J. Hsu, "An integrated low-noise sensing circuit with efficient Bias stabilization for CMOS MEMS capacitive accelerometers," *IEEE Transactions on Circuits and Systems I: Regular Papers*, vol. 58, no. 11, pp. 2661–2672, Nov. 2011, doi: 10.1109/TCSI.2011.2142990.

[22] T. B. Gabrielson, "Mechanical-thermal noise in micromachined acoustic and vibration sensors," *IEEE Transactions on Electron Devices*, vol. 40, no. 5, pp. 903–909, May 1993, doi: 10.1109/16.210197.

[23] W. Kuehnel, "Modelling of the mechanical behaviour of a differential capacitor acceleration sensor," *Sensors and Actuators A: Physical*, vol. 48, no. 2, pp. 101–108, May 1995, doi: 10.1016/0924-4247(94)00983-O.

[24] M. Lemkin and B. E. Boser, "A three-axis micromachined accelerometer with a CMOS position-sense interface and digital offset-trim electronics," *IEEE Journal of Solid-State Circuits*, vol. 34, no. 4, pp. 456–468, Apr. 1999, doi: 10.1109/4.753678.

[25] B. V Amini and F. Ayazi, "A 2.5-V 14-bit /spl sigma//spl delta/ CMOS SOI capacitive accelerometer," *IEEE Journal of Solid-State Circuits*, vol. 39, no. 12, pp. 2467–2476, Dec. 2004, doi: 10.1109/JSSC.2004.837025.

BIOGRAPHIES OF AUTHORS

Anwer Sabah Ahmed is a lecturer at Engineering Technical College, Al-Njaf – Al-Furat Al-Awsat Technical University. He obtained his B.Sc. degree in electrical engineering from the Technical College of Najaf Al-Furat al-Awsat University in 2002. Then, he obtained his M.Sc. degree in electrical engineering, electronics, and communications from the University of Technology Iraq, Baghdad. His fields of interest include electronics, power electronics, coding, security, IoT, control, optimization, and wireless communications. He can be contacted at anwar.altamimi@student.uobabylon.edu.iq or Inj.anw@atu.edu.iq.

Qais Al-Gayem received a B.S. degree in Electrical and Electronic Engineering from the University of Babylon, and an M.S. degree in Electronic Engineering from the University of Technology, Iraq, in 1999 and 2001, respectively. Between 2002 and 2008, he worked as a lecturer in the Electrical Department, University of Babylon, Iraq. Following this, he studied for his Ph.D. in the Engineering Department, at Lancaster University, UK, and graduated in 2012. He is currently an assistant professor at the Electrical Department, Faculty of Engineering, University of Babylon, Iraq. His research interests include built-in self-test (BIST) of MEMS and NEMS, health monitoring, and dependability in bio-fluidic microsystems. He can be contacted at eng.qais.karem@uobabylon.edu.iq.